Influences of Bonding Materials on the Accuracy of Fibre Bragg Grating Strain Measurements

Wei Zhang, Weimin Chen, Yuejie Shu, Xiaohua Lei

7th European Workshop on Structural Health Monitoring
July 8-11, 2014. La Cité, Nantes, France

INFLUENCES OF BONDING MATERIALS ON THE ACCURACY OF FIBRE BRAGG GRATING STRAIN MEASUREMENTS

Wei Zhang, Weimin Chen*, Yuejie Shu, and Xiaohua Lei

Sensors and Instruments Research Center, the Key Lab. for Optoelectronic Technology & Systems of Ministry of Education, College of Optoelectronic Engineering, Chongqing University, Chongqing, 400044, China

wmchen0802@126.com

ABSTRACT

To achieve accurate strain measurements using fibre Bragg gratings (FBGs), both the sensing and wavelength demodulation accuracy are worth considering. Due to the indispensability, influences of bonding materials on the measurement accuracy need to be clarified. To analyze the sensing accuracy of the FBG strain sensor, a simplified longitudinal strain transmission model is established to discuss the transfer coefficient issue. Results indicate that hard bonding materials can enhance the sensing accuracy by high strain sensitivity. But on the other hand, asymmetric transversal stress model reveals that hard bonding materials can lead to the distortion of the spectrum in a large load condition. Then, effects of distorted spectra on the wavelength demodulation accuracy are studied by the simulation. The simulation shows that distorted spectra can reduce the wavelength demodulation accuracy markedly. It can be concluded that to improve the accuracy of strain measurements, hard bonding materials are suitable for small strain measurements, and relatively soft bonding materials are better options for large strain measurements.

KEYWORDS : *fibre Bragg grating, accuracy, bonding materials, strain measurement, wavelength demodulation.*

1 INTRODUCTION

The FBG, owing to its distinguished features, such as relatively small physical dimension, and the ability to be multiplexed, is regarded as an ideal sensing element for strain measurements in Structural Health Monitoring[1-3]. According to the strain measurement principle of the FBG, wavelength shift of the FBG is related to the strain applied on it. The measured strain value is generally obtained by interpreting the wavelength shift from the spectral response of the FBG. So, to measure the strain accurately, the FBG, first, need to sense the strain as accurately as possible, and translate it into the shift of the spectrum. Then, it has to employ a suitable algorithm to recognize the wavelength shift from the spectrum provided by the FBG.

But being fragile and easily damaged, it is impractical to apply the bare FBG to engineering application. It must be packaged into a FBG strain sensor as a whole sensing unit to suit the harsh engineering application environment. By dissecting a FBG strain sensor, it can be seen that the FBG is bonded onto the packaging structure by the bonding material. The bonding material serves as the middle strain transmission medium, delivering the strain from the packaging structure to the FBG. In the strain transmission process, the bonding material converts part of the energy into its shear deformation, thus the strain sensed by the FBG is inconsistent with that of the packaging structure. As a consequence, the strain sensing accuracy of the FBG sensor is highly dependent on characteristics of the bonding material. To analyze strain transfer characteristics of the FBG sensor, some scholars have proposed different theoretical models based on the shear-lag theory [4-6]. Although these models are different, they can come to the same conclusion that thin bonding

thickness and long bonding length contribute to the strain sensing accuracy. This conclusion is benefit for the optimization of the physical dimension of the bonding layer, which is a considerable issue for the fabrication of the FBG strain sensor.

To further enhance the strain sensing accuracy, some bonding materials harder than the common used epoxy and acrylic adhesives, like alumina[7], Ag-Cu alloy[8], soldering tin[9], and zinc[10], are applied. Hard bonding materials are perceived as good candidates for replacing the organic adhesives to improve the strain sensing accuracy. But on the other hand, we found that it is easier for hard bonding materials to cause stress-induced birefringence effect within FBGs due to asymmetric transversal stresses of loaded FBG strain sensors[10]. Large birefringence will cause the distortion of the spectrum. Distorted spectrum may further reduce the wavelength demodulation accuracy. In other words, adopting hard bonding materials may not achieve the purpose of enhancing the accuracy of strain measurement using the FGB. In this article, we will investigate influences of bonding materials on the accuracy of FBG strain measurement comprehensively, hoping to provide guidance for the fabrication of FBG strain sensors.

2 STRAIN MEASUREMENT PRINCIPLE OF THE FBG

For an undisturbed FBG, it reflects incident light in a narrow band single-peaked spectrum. The Bragg wavelength of the spectrum satisfies the Bragg condition as follows[1]

$$\lambda_B = 2 n_{eff} \Lambda \tag{1}$$

where λ_B is the Bragg wavelength, n_{eff} is the average effective index of refraction of the core and Λ is the periodicity of the grating. When the FBG is disturbed by the external parameter, e.g. the strain or temperature, the Bragg wavelength will shift. Assuming that the temperature is constant, the FBG will provide a linear response based on the measurement of wavelength shift $\Delta\lambda_B$ due to the strain of the FBG. The linear response function of the average strain sensed by FBG ε_{FBG} is represented as

$$\frac{\Delta\lambda_B}{\lambda_B} = [1 - \frac{1}{2} n_{eff}^2 (p_{12} - \nu(p_{11} + p_{12}))]\varepsilon_{FBG} \tag{2}$$

where p_{11} and p_{12} are photo-elastic constants and ν is the Poisson's ratio of the fibre. By measuring the wavelength shift $\Delta\lambda_B$, the external strain can be determined.

3 INFLUENCES OF BONDING MATERIALS ON SENSING ACCURACY OF FBG STRAIN SENSORS

3.1 Model of the loaded FBG strain sensor

To apply FBGs to strain measurements, bare FBGs can be packaged into various shaped FBG strain sensors to meet requirements of different applications. Based on shapes of packaging structures, they can be mainly classified into two types: tubular and slice-packaged FBG strain sensors. Since slice-packaged FBG strain sensors are more frequently used, the following analysis is chiefly based on them.

Figure 1 shows some slice-packaged FBG strain sensors available on the market and in the laboratories [7, 11]. They are installed on surfaces of the measured structures in applications. Shapes of these sensors seem different, but they can be simplified into a similar configuration as shown in Figure 2 (a) and (b). The installed FBG strain sensor absorbs the strain of the measured structure through the installation layer in the first step, and then the strain causes the deformation of the packaging structure. Inside the sensor, the bonding layer is unavoidable as it provides the connection for the FBG and the packaging structure. Due to the direct action on the FBG, the bonding material has great potentials to influence the spectral response. To discuss effects of the bonding material on the spectral response of the sensor, the whole strain field exerted on the FBG is decomposed into longitudinal and transversal strain fields as shown in Figure 2 (c) and (d) respectively; and it will be analyzed in the following two sections.

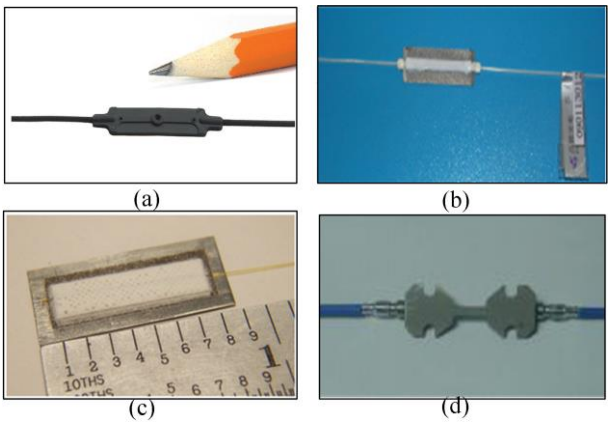

Figure 1: Slice-packaged FBG strain sensors (a) os3200 Optical Strain Gage made by Micro Optics (b) FBGS615N1FBG Strain Gage made by Beijing Pi-Optics Co., Ltd (c) FBG using sprayed alumina onto a metal shim (d) FBG strain sensor encapsulated by mental slice

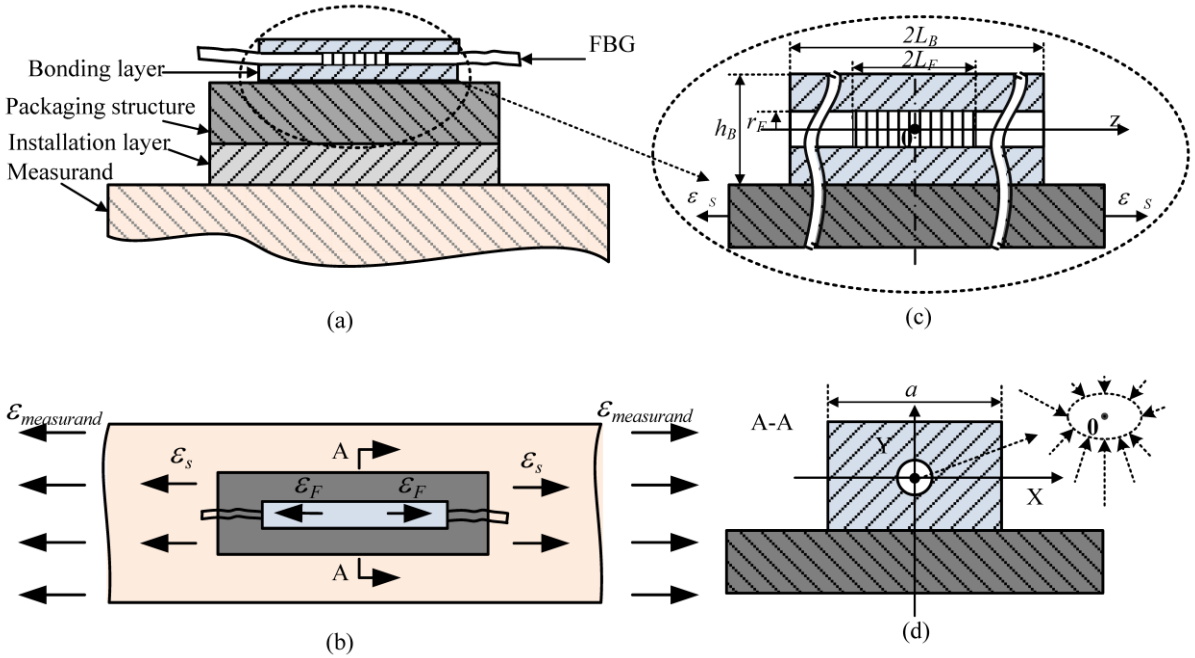

Figure 2: (a) Front view of a surface-installed FBG strain sensor (b) top view of a surface-installed FBG strain sensor (c) simplified longitudinal strain transmission model for the FBG strain sensor (d) simplified asymmetric transversal strain model for the FBG strain sensor

3.2 Mechanical analysis of the longitudinal strain field

Assume that the packaging structure stretches uniformly and its strain is ε_S as indicated in Figure 2 (c), the final longitudinal strain distributed along the FBG can be written as[5]:

$$\varepsilon_F(z) = \varepsilon_S[1 - \frac{\cosh(\eta z)}{\cosh(\eta L_B)}], \qquad z \in [-L_B, L_B] \tag{3}$$

where L_B is the half bonding length of the bonding layer, η is the strain lag parameter given by

$$\eta = \sqrt{\frac{8G_B}{E_F(3h_B - 2r_F)(h_B + 2r_F)}} \tag{4}$$

where subscripts B and F stand for the bonding layer and the FBG, and G, h and r denote shear modulus, thickness and radius, respectively.

To facilitate discussions, we define a function of strain transfer coefficient $K(z)$ as

$$K(z) = \frac{\varepsilon_F(z)}{\varepsilon_S} = 1 - \frac{\cosh(\eta z)}{\cosh(\eta L_B)}, \qquad z \in [-L_B, L_B] \tag{5}$$

According to Equation (5), Figure 3 plots the function *K (z)* of different shear modulus G_B under different bonding length $2L_B$. In fact, this graph implies the distribution of longitudinal strain exerted on the grating. From this graph, it can be concluded that the bonding length $2L_B$ should be as long as possible for a bonding material with low shear modulus; otherwise, a distorted spectrum may appears as a consequence of the non-uniform strain field along the grating. From another perspective, it indicates that high shear modulus bonding material is conducive to ensuring a uniform strain field for the FBG strain sensor.

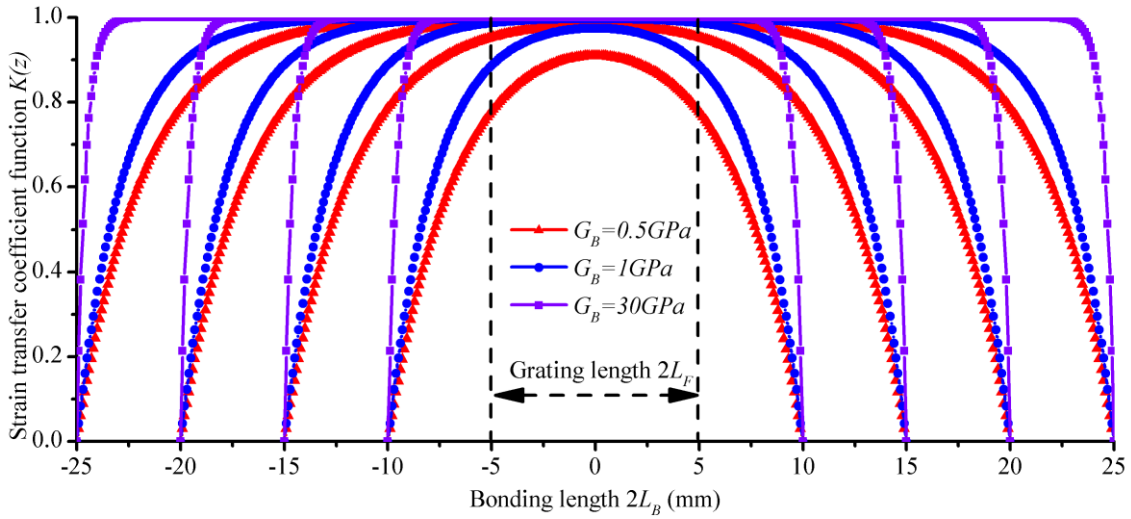

Figure 3: Function *K (z)* of different shear modulus G_B under different bonding length $2L_B$. (Parameter values set in this simulation are E_F=74Gpa, r_F=62.5um, h_B=0.4mm)

Supposing an acceptable longitudinal strain field is guaranteed by reasonable dimensions of the bonding layer; then, the average strain sensed by the FBG ε_{FBG} is another issue worth considering, as it decides the wavelength shift $\Delta\lambda_B$ of the spectrum. Based on Equation (3), ε_{FBG} can be calculated by

$$\varepsilon_{FBG} = \frac{\int_{-L_B}^{L_B} \varepsilon_F(z)dz}{2L_B} = [1 - \frac{\sinh(\eta L_B)}{\eta L_B \cosh(\eta L_B)}]\varepsilon_S \tag{6}$$

To reflect the FBG strain sensor's sensing accuracy, we define its strain sensitivity K_{sensor} as

$$K_{sensor} = \frac{\Delta\lambda_B}{\varepsilon_S} \tag{7}$$

And we can find K_{sensor} by substituting Equation (6) into Equation (2)

$$K_{sensor} = \lambda_B[1 - \frac{1}{2}n_{eff}^2(p_{12} - \nu(p_{11} + p_{12}))][1 - \frac{\sinh(\eta L_B)}{\eta L_B \cosh(\eta L_B)}] \tag{8}$$

The relationship of the bonding material's shear modulus G_B to the strain sensitivity K_{sensor} is illustrated by Figure 4. It clearly shows that the high shear modulus bonding material is able to increase the strain sensitivity, which is productive to the sensor's sensing accuracy. An instance is that the metal material, e.g. zinc, is a good option for high sensing accuracy comparing with the organic material, e.g. epoxy.

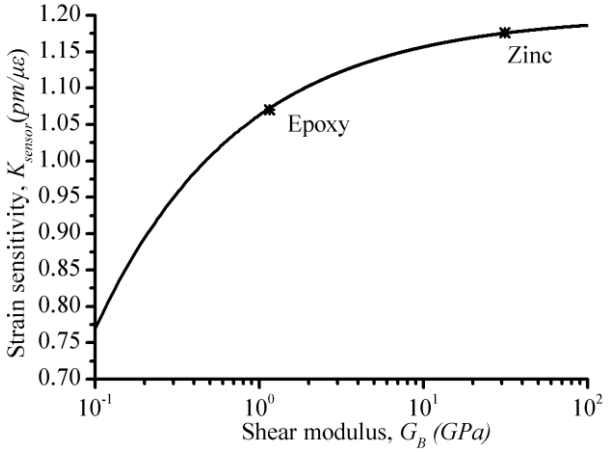

Figure 4: Relationship of the bonding material's shear modulus to the FBG sensor's strain sensitivity (Parameter values set in this simulation are L_B=20mm, $\lambda_B[1-n^2_{eff}(p_{12}-v(p_{11}+p_{12}))]$=1.2 pm/ $\mu\ \varepsilon$)

3.3 Mechanical analysis of the transversal strain field [10]

When the FBG strain sensor stretches longitudinally, the bonding material shrinks transversally at the same time. This shrinkage causes asymmetrical transversal forces onto the FBG as shown in Figure 2 (d). As a consequence, refractive index changes of the two directions Δn_x , Δn_y are different, making it satisfy the condition of stress-induced birefringence[12]. Correspondingly, the FBG reflects two single-peaked spectra at two Bragg wavelengths λ_x and λ_y , resulting in the expansion of bandwidth as shown in Figure 5.

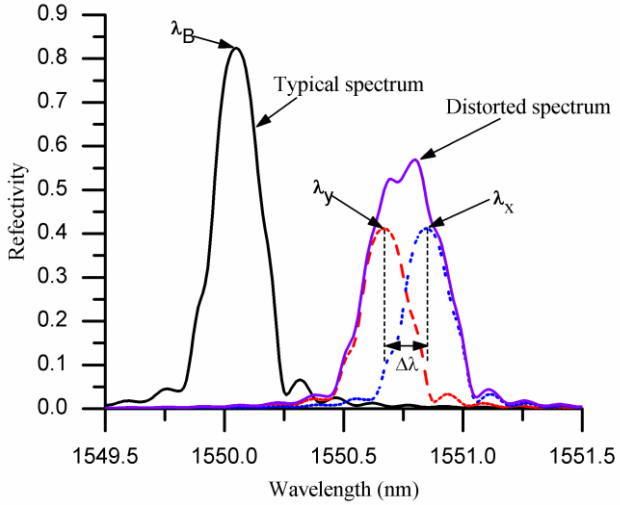

Figure 5: Typical spectrum and distorted spectrum caused by stress-induced birefringence

The magnitude of stress-induced birefringence is closely related to the material properties of the bonding layer. Figure 6 simulates changes of reflected spectra caused by different bonding materials as functions of the longitudinal strain. It can be seen that the harder bonding material, zinc, will lead to obvious distortion of the spectrum under a large load condition. Interestingly, the relatively soft bonding material, epoxy, can keep a good quality of the spectrum in a large strain variation range.

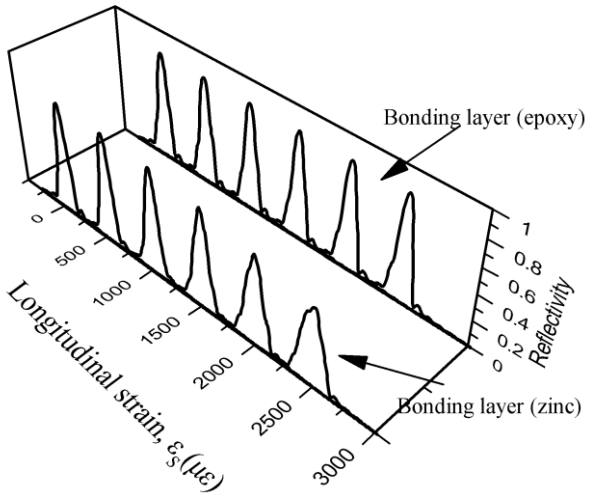

Figure 6: Changes of reflected spectra caused by different bonding materials as functions of the longitudinal strain

4 INFLUENCES OF DISTORTED SPECTRA ON WAVELENGTH DEMODULATION ACCURACY

4.1 Wavelength demodulation algorithms

To get the measured strain, the wavelength shift needs to be demodulated from the obtained spectrum from the FBG. There are different wavelength demodulation algorithms[13], and the most common used methods are maximum algorithm, centroid algorithm and least squares fitting algorithm.

The maximum algorithm is based on the search for the wavelength with the highest amplitude in the reflected spectrum. The centroid algorithm determines the wavelength shift $\Delta \lambda_B$ by calculating the centroid wavelength shift $\Delta \lambda_c$ of the spectrum, and centroid wavelength is calculated by

$$\lambda_c = \frac{\sum_{i=1}^{N} \lambda_i A_i}{\sum_{i=1}^{N} A_i} \tag{9}$$

where λ_i are the measured wavelengths and A_i are the corresponding reflected powers. The least squares fitting method is implemented by minimizing the squared errors using Gauss-Newton algorithm. A second order polynomial is used for the least squares fitting algorithm in the following analysis.

4.2 Decline of wavelength demodulation accuracy

As mentioned in section 3.3, a distorted spectrum may occur if the bonding material is improper. In fact, the final obtained spectrum is filled with random fluctuations as demonstrated in Figure 7, accounting for the system noise. For the distorted spectrum, as it can't maintain a single peak, it would further increase the difficulty of accurate wavelength demodulation. To study effects of distorted spectra shown in Figure 6 on the wavelength demodulation accuracy, the bandwidth is used to characterize degrees of distortions. Behaviours of algorithms are given in Figure 8.

It can be seen from Figure 8 that wavelength demodulation accuracy decreases with the increase of the bandwidth. Also, when the bandwidth of distorted spectrum increases to two times of that of the undistorted spectrum, the measurement error can achieve as much as 80pm. So, it is tough to achieve high-accuracy strain measurement once the improper bonding material leads to serious distortion of the spectrum.

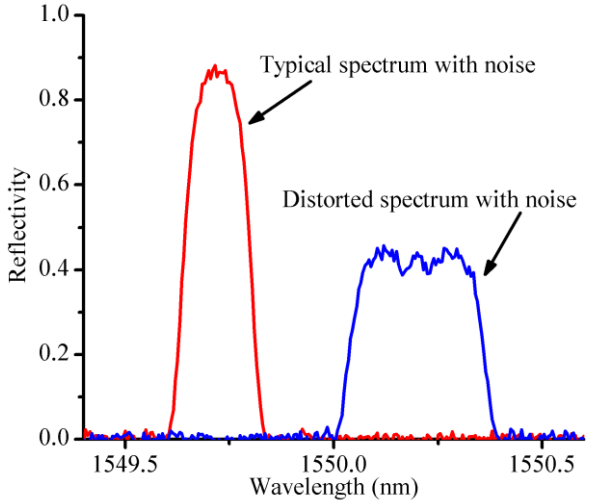

Figure 7: Typical spectrum with noise and distorted spectrum with noise

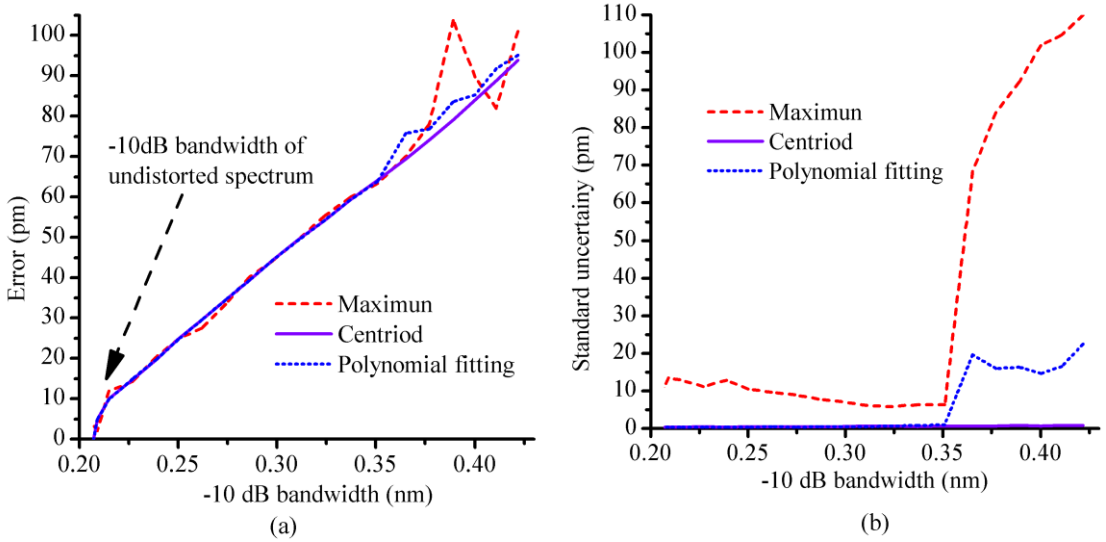

Figure 8: (a) Influence of distorted spectra on the wavelength demodulation error (b) Influence of distorted of spectra on the wavelength demodulation uncertainty

5 CONCLUSION

Because the packaging of bare FBG is unavoidable, the bonding material plays a key role in deciding the accuracy of practical strain measurements. Stress conditions of the loaded strain sensor are analyzed roundly in this article. According to the function of strain transfer coefficient, we find that to assure a uniform longitudinal strain field along the grating, the bonding length of soft materials need to be longer than that of hard materials. In addition, the relationship of the strain sensitivity to the shear modulus of the bonding material is given; and it indicates that it is beneficial to adopt hard bonding materials to enhance the sensing accuracy. However, due to the effect of stress-induced birefringence, the distorted spectrum is more likely to appear in a large strain condition if an improper hard bonding material is applied. For these common used wavelength demodulation algorithms, distorted spectra are counterproductive to their demodulation accuracy. Therefore, to enhance the strain measurement accuracy, hard bonding materials are advisable for fabricating FBG strain sensors applied in small strain measurements. With regard to large strain measurements, relatively soft bonding materials are encouraged.

ACKNOWLEDGMENT

This work was supported by the National Natural Science Foundation of China (No. 51078369) and the National Natural Science Foundation of China (No. 50975301).

REFERENCES

[1] A. Othonos. Fiber Bragg gratings. *Review Of Scientific Instruments,* 68(12):4309-4341, 1997.

[2] M. Majumder, T. K. Gangopadhyay, A. K. Chakraborty, K. Dasgupta, and D. K. Bhattacharya. Fibre Bragg gratings in structural health monitoring - Present status and applications. *Sensors and Actuators A,* 147(1):150-164, 2008.

[3] R. P. Beukema. Embedding technologies of FBG sensors in composites: Technologies, applications and practical use. *Proceedings of the 6th European Workshop on Structural Health Monitoring,*Tu.4.C.4: 341-348, July 2012.

[4] F. Ansari and L. B. Yuan. Mechanics of bond and interface shear transfer in optical fiber sensors. *Journal of Engineering Mechanics,* 124(4):385-394, 1998.

[5] J. L. Li, Z. Zhou, and J. P. Ou. Interface strain transfer mechanism and error modification for adhered FBG strain sensor. *Proceedings of SPIE,*5851: 278-287, June 2005.

[6] D. S. Li, H. N. Li, L. Ren, and G. B. Song. Strain transferring analysis of fiber Bragg grating sensors. *Optical Engineering,* 45(2): 024402, 2006.

[7] V. P. Wnuk, A. Mendez, S. Ferguson, and T. Graver. Process for mounting and packaging of fiber Bragg grating strain sensors for use in harsh environment applications. *Proceedings of SPIE,*5758: 46-53, May 2005.

[8] S. Sandlin, T. Kinnunen, J. Ramo, and M. Sillanpaa. A simple method for metal re-coating of optical fibre Bragg gratings. *Surface & Coatings Technology,* 201(6):3061-3065, 2006.

[9] M. S. Muller, L. Hoffmann, T. Lautenschlager, and A. W. Koch. Soldering fiber Bragg grating sensors for strain measurement. *Proceedings of SPIE,*7004: 70040B, June 2008.

[10] W. Zhang, W. M. Chen, Y. J. Shu, X. H. Lei, and X. M. Liu. Effects of bonding layer on the available strain measuring range of fiber Bragg gratings. *Applied Optics,* 53(5):885-891, 2014.

[11] Z. Zhou, W. G. Thomas, and J. P. Ou. Techniques of advanced FBG sensors: manufacturing, demodulation, encapsulation and their application in the structural health monitoring of bridges. *Pacific Science Review,* 5(1):116-121, 2003.

[12] R. Gafsi and M. A. El-Sherif. Analysis of induced-birefringence effects on fiber Bragg gratings. *Optical Fiber Technology,* 6(3):299-323, 2000.

[13] L. Negri, A. Nied, H. Kalinowski, and A. Paterno. Benchmark for Peak Detection Algorithms in Fiber Bragg Grating Interrogation and a New Neural Network for its Performance Improvement. *Sensors,* 11(4):3466-3482, 2011.